

*** The European Physical Society Conference on High Energy Physics
(EPS-HEP2021), ***

*** 26-30 July 2021 ***

*** Online conference, jointly organized by Universität Hamburg and the
research center DESY ***

1 CKM parameter measurement with semileptonic 2 B_s decays at LHCb

3 **Anna Lupato**^{a,*}

4 *On behalf of LHCb Collaboration*

5 ^a*The University of Manchester, Manchester, UK*

6 *E-mail: anna.lupato@cern.ch*

The long standing discrepancy between determinations of the CKM matrix element V_{ub} obtained from exclusive and inclusive semileptonic B decays are at the level of 3 standard deviations. This discrepancy continues to challenge our understanding of the semileptonic decays on both the theoretical and experimental sides. Exclusive semileptonic B_s decays are in principle under good theoretical control and provide complementary information with respect to the B-factories in this sector. The article reports the observation of the decay $B_s^0 \rightarrow K^- \mu^+ \nu_\mu$ using 2fb^{-1} of data recorded in 2012 by the LHCb detector. Using the measurement of the $B_s^0 \rightarrow K^- \mu^+ \nu_\mu$ branching fraction relative to the well known $B_s^0 \rightarrow D_s^- \mu^+ \nu_\mu$ decay, and the most recent theoretical knowledge of the relevant B_s decays form factors, the ratio of CKM matrix elements V_{ub}/V_{cb} is extracted, with a precision competitive with the existing measurements.

*Speaker

1. The CKM $|V_{xb}|$ parameter

In order to test the unitarity of the CKM matrix and precisely measure the amount of CP violation in the quark sector, the parameters of the CKM matrix must be constrained. The CKM parameters can be constrained by performing measurements of observables sensitive to the magnitudes of the CKM matrix elements. Since $|V_{xb}|$ ($x = u, c$) are the least well known of the CKM matrix elements it is the dominant limiting factor when drawing CKM unitary triangles. An improved uncertainty on $|V_{xb}|$ improve the global precision of fits to the CKM unitary triangles and test the unitarity of the CKM matrix. Non unitarity of the CKM matrix would be indicative of new physics beyond the standard model, so $|V_{xb}|$ measurements provide a crucial input on indirect searches of New Physics.

2. Inclusive and exclusive measurements

The matrix elements can be determined from inclusive and exclusive semileptonic decays of a B hadron. In exclusive measurements a specific meson is reconstructed, instead for the inclusive decays $B \rightarrow X_{u/c} \mu \nu_\mu$ a sum over all possible hadronic final states is performed. Such measurements were performed by the B factories using B^0 and B^+ mesons as well as by LEP experiments. A discrepancy between inclusive and exclusive measurements of approximately three standard deviations is observed, a long-standing puzzle in flavour physics [1].

3. First observation of the decay $B_s^0 \rightarrow K^- \mu^+ \nu_\mu$ and a measurement of V_{ub}/V_{cb}

The world average of the exclusive V_{ub} results is dominated by $B^0 \rightarrow \pi^- l^+ \nu_l$ measurements [1]. A different approach was used to extract the ratio V_{ub}/V_{cb} for the first time at a hadron collider by LHCb using exclusive semileptonic Λ_b decays [2] and gave the ratio $V_{ub}/V_{cb} = 0.079 \pm 0.006$. This article reports the first observation of the decay $B_s^0 \rightarrow K^- \mu^+ \nu_\mu$, the measurement of its branching fraction and of the ratio V_{ub}/V_{cb} with $B_s^0 \rightarrow D_s^- \mu^+ \nu_\mu$ as a normalization channel. The data sample consists of pp collisions recorded by the LHCb detector in 2012 at a center-of-mass energy of 8 TeV corresponding to 2fb^{-1} of integrated luminosity.

$B_s^0 \rightarrow K^- \mu^+ \nu_\mu$ and $B_s^0 \rightarrow D_s^- \mu^+ \nu_\mu$ decays are formed by combining a muon with a kaon or a D_s^- candidate reconstructed through the decay $D_s^- \rightarrow K^+ K^- \pi^-$. The trigger and initial selection requirements are chosen to be similar between these two modes. Events are retained due to the presence of a high- p_T muon, where p_T is the momentum component transverse to the beam and partially reconstructed B decays are selected by combining a track or a D_s^- candidate with a well identified muon candidate. The selection includes requirements on the track kinematics and quality, particle identification, as well as on the B_s^0 candidate kinematics and decay topology. The obtained samples for each of the decays include background contributions dominated by b -hadron decays with additional tracks or neutral particles in the final state.

46 For the $K^-\mu^+$ combinations, the main background originates from $H_b \rightarrow \mu^+H_c(\rightarrow$
 47 $K^-)X'$, where $H_{b,c}$ represents a hadron containing a b or c quark and X' the possible
 48 unreconstructed particles. The secondary contributions of background are the decays to
 49 excited K^* resonances, $B_s^0 \rightarrow K^{*-}(\rightarrow K^-\pi^0)\mu^+\nu_\mu$, and charmonium modes $B \rightarrow [c\bar{c}](\rightarrow$
 50 $\mu^+\mu^-)K^-X$, where $[c\bar{c}] = J/\psi, \psi(2S)$. Other sources arise from b -hadron decays where a
 51 track is misidentified as a kaon or a muon, and random combinations of a muon and a kaon.

52 The main and irreducible source of background in the $D_s^-\mu^+$ combinations is formed by
 53 $B_s^0 \rightarrow D_s^{*-}(\rightarrow D_s^-\gamma)$ decays. Additional contributions include decays to higher excitations
 54 of the D_s^- meson, double-charm decays of the type $B_{u,d,s} \rightarrow D_sDX$ and semitauonic $B_s^0 \rightarrow$
 55 $D_s^-\tau^+\nu_\tau$ decays.

56 To suppress background, the $K^-\mu^+$ and $D_s^-\mu^+$ candidates are required to be isolated
 57 from other tracks in the event: a multivariate algorithm (MVA) is trained to determine if
 58 a given track originates from the candidate or from the rest of the event (isolation MVA).
 59 Two boosted decision tree (BDT) classifiers are used sequentially for the $K^-\mu^+$ candidates
 60 to further reduce the remaining background. BDT classifier to isolate the signal from
 61 additional charged tracks is trained against the main background components using, in
 62 addition to the isolation MVA output, invariant masses formed by the least isolated track
 63 with respect to each of the muon or the kaon, and variables related to the B_s^0 , K^- and
 64 μ^- kinematics. A second BDT classifier involves kinematic variables of the K^- and B_s^0
 65 candidates, the B_s^0 vertex position and quality, the invariant mass formed by the signal
 66 kaon and any π^0 meson and the asymmetry between the kaon momentum and an average
 67 momentum direction formed by neutral particles in the vicinity of the kaon.

68 The B_s^0 momentum in a semileptonic decay can be determined only by a two-fold
 69 ambiguity. This is resolved by choosing the solution that is most consistent with the B_s^0
 70 momentum predicted by a linear regression method which exploits the information from
 71 the B_s^0 reconstructed flight directions [4].

In order to extract the signal yields a binned maximum likelihood fit to the B_s^0 corrected
 mass [3] has been performed in two interval of $B_s^0 \rightarrow K^-$ momentum transfer q^2 , respectively
 above and below $7\text{GeV}^2/c^4$, which are chosen to contain approximately the same expected
 signal yields. The corrected mass is defined as

$$m_{corr} = \sqrt{m_{Y\mu}^2 + p_\perp^2/c^2} + p_\perp/c,$$

72 where $m_{Y\mu}$ the invariant mass of the $Y\mu$ pair, with $Y = K^-$ or D_s^- , and p_\perp is the
 73 momentum of this pair transverse to the B_s^0 flight direction, defined as the vector between
 74 the positions of the primary pp collision vertex and the B_s^0 decay vertex. If the only missing
 75 particle is a neutrino the corrected mass distribution will peak at the B_s^0 mass.

76 About the 90% of combinatorial background for the $B_s^0 \rightarrow K^-\mu^+\nu_\mu$ has been reduced
 77 by requiring that the opening angle between the directions of the K^- and μ^- candidates in
 78 the plane transverse to the pp collision axis to be less than 90 degrees. The signal template
 79 for the m_{corr} is obtained from simulation, while the shapes for the background components
 80 are derived from either simulation or data control samples.

81 For the $B_s^0 \rightarrow D_s^-\mu^+\nu_\mu$ decay, a fit to the invariant mass of the $D_s^- \rightarrow K^+K^-\pi^-$
 82 candidates is performed in 40 intervals of m_{corr} from 3000 to 6500 MeV/c^2 , in order to

83 subtracts the background originating from combinations of random kaon and pion tracks
 84 and provide the D_s . The obtained m_{corr} distribution is then fitted to extract the $B_s^0 \rightarrow$
 85 $D_s^- \mu^+ \nu_\mu$ signal yields. The signal template for the m_{corr} is obtained from simulation,
 86 while the shapes for the background components are derived from either simulation or
 87 data control samples. Figure 1 shows the corrected mass distributions of the signal and
 88 normalization candidates with the binned maximum-likelihood fit projections overlaid. The
 89 resulting yields for the $B_s^0 \rightarrow K^- \mu^+ \nu_\mu$ decays are $N_K = 6922 \pm 285$ and $N_K = 6399 \pm 370$
 90 respectively for $q^2 < 7 \text{ GeV}^2/c^4$ and $q^2 > 7 \text{ GeV}^2/c^4$, while the $B_s^0 \rightarrow D_s^- \mu^+ \nu_\mu$ yields are
 91 $N_{D_s} = 201450 \pm 5200$. The largest systematic uncertainty originates from the fit templates
 92 and is evaluated by varying the shape of the fit components according to alternative models
 93 and also by modifying within its uncertainty the mixture of exclusive decays representing
 some of the background contributions.

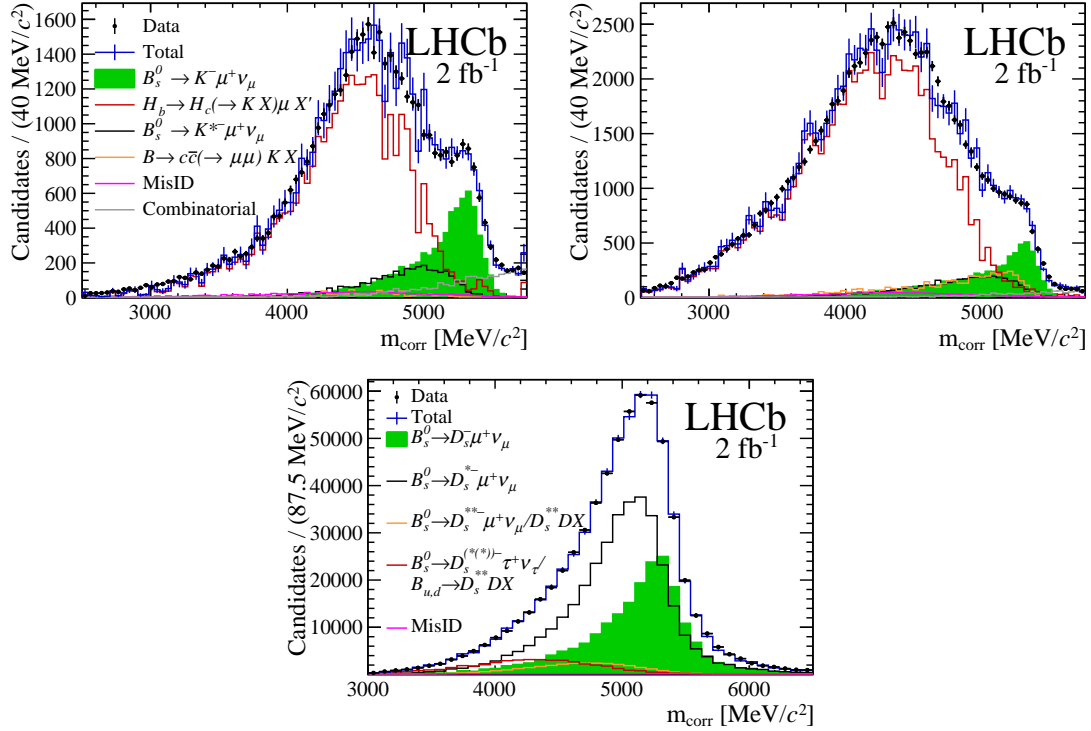


Figure 1: Distribution of m_{corr} for (top) the signal $B_s^0 \rightarrow K^- \mu^+ \nu_\mu$, with (left) $q^2 < 7 \text{ GeV}^2/c^4$ and (right) $q^2 > 7 \text{ GeV}^2/c^4$, and (bottom) the normalization $B_s^0 \rightarrow D_s^- \mu^+ \nu_\mu$ channel. The points represent data, while the resulting fit components are shown as histograms.

94

The measured ratio is therefore:

$$R_{BF} = \frac{\mathcal{B}(B_s^0 \rightarrow K^- \mu^+ \nu_\mu)}{\mathcal{B}(B_s^0 \rightarrow D_s^- \mu^+ \nu_\mu)} = \frac{N_K}{N_{D_s}} \frac{\epsilon_{D_s}}{\epsilon_K} \times \mathcal{B}(D_s^- \rightarrow K^+ K^- \pi^-), \quad (1)$$

95 where ϵ_i are the overall efficiencies for the signal and normalization channels and $\mathcal{B}(D_s^- \rightarrow$
 96 $K^+ K^- \pi^-) = (5.39 \pm 0.15)\%$ [5]. The ratio is computed for bin $q^2 < 7 \text{ GeV}^2/c^4$ or low, $q^2 > 7$
 97 GeV^2/c^4 or high, and integrated:

$$\begin{aligned}
R_{BF}(\text{low}) &= (1.66 \pm 0.08(\text{stat}) \pm 0.07(\text{syst}) \pm 0.05(D_s)) \times 10^{-3}, \\
R_{BF}(\text{high}) &= (3.25 \pm 0.21(\text{stat})_{-0.17}^{+0.16}(\text{syst}) \pm 0.09(D_s)) \times 10^{-3}, \\
R_{BF} &= (4.89 \pm 0.21(\text{stat})_{-0.21}^{+0.20}(\text{syst}) \pm 0.14(D_s)) \times 10^{-3},
\end{aligned}$$

where (D_s) stands for the error on the D_s decay branching fraction. The absolute branching fraction is then available using:

$$\mathcal{B}(B_s^0 \rightarrow K^- \mu^+ \nu_\mu) = R_{BF} \times \tau_{B_s} \times |V_{cb}|^2 \times FF_{D_s}, \quad (2)$$

where the following external inputs are used: $|V_{cb}| = (39.5 \times 0.9) \times 10^{-3}$ [5], the lifetime $\tau_{B_s} = 1.515 \pm 0.004\text{ps}$ [5] and $FF_{D_s} = 9.15 \pm 0.37$ based on a recent LQCD computation [6]. It results:

$$\mathcal{B}(B_s^0 \rightarrow K^- \mu^+ \nu_\mu) = (1.06 \pm 0.05(\text{stat}) \pm 0.08(\text{syst})) \times 10^{-4}. \quad (3)$$

The ratio of branching fractions can be written as

$$\frac{|V_{ub}|}{|V_{cb}|} = \sqrt{R_{BF} \times \frac{FF_{D_s}}{FF_K}}, \quad (4)$$

so the measured ratio of branching fractions is combined with theoretical inputs from Lattice QCD and Light-Cone Sum Rules allowing to be determined V_{ub}/V_{cb} . Different FF_K predictions have been used in the two q^2 bins to exploit the best precision reachable. In fact, lattice QCD predictions provide a precise determination of the form factors at low recoil transfer [7] [8] [9], while calculations from QCD light-cone sum rules are most precise at large recoil [10]. The obtained values are :

$$\begin{aligned}
\frac{|V_{ub}|}{|V_{cb}|}(q^2 < 7 \text{ GeV}^2/c^4) &= 0.0607 \pm 0.0015(\text{stat}) \pm 0.0013(\text{syst}) \pm 0.0008(D_s) \pm 0.0030(FF) \\
\frac{|V_{ub}|}{|V_{cb}|}(q^2 > 7 \text{ GeV}^2/c^4) &= 0.0946 \pm 0.0030(\text{stat})_{-0.0025}^{+0.0024}(\text{syst}) \pm 0.0013(D_s) \pm 0.0068(FF)
\end{aligned}$$

where the latter two uncertainties are from the D_s branching fraction and the form factor integrals.

4. Conclusion

This report presented the first observation and measurement of the branching ratio of the $B_s^0 \rightarrow K^- \mu^+ \nu_\mu$ decays. Moreover it presented a new measurement of V_{ub}/V_{cb} in two q^2 bins. A discrepancy between the low and high bin ratio has been found and as you can see in Fig.4, only the high q^2 bin ratio is compatible with the previous world average for exclusive V_{ub}/V_{cb} measurement. This results improve both the averages of the exclusive measurements in the (V_{cb}, V_{ub}) plane and the precision on the least known side of the CKM unitarity triangle

References

- [1] Y. S. Amhis *et al.* [HFLAV], Eur. Phys. J. C **81** (2021) no.3, 226 doi:10.1140/epjc/s10052-020-8156-7 [arXiv:1909.12524 [hep-ex]].

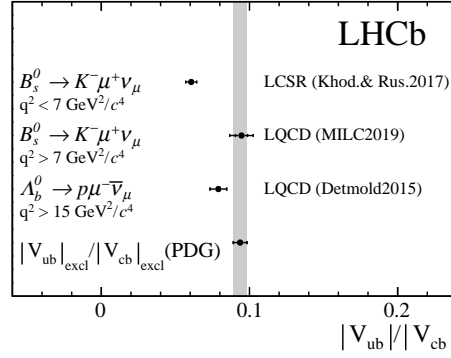


Figure 2: V_{ub}/V_{cb} ratio: measurement presented in this report, previous LHCb measurement based on $\Lambda_b^0 \rightarrow p\mu^-\bar{\nu}$ decays [2] and PDG average [5]

- 122 [2] R. Aaij *et al.* [LHCb], *Nature Phys.* **11** (2015), 743-747 doi:10.1038/nphys3415
 123 [arXiv:1504.01568 [hep-ex]].
- 124 [3] K. Abe *et al.* [SLD], *Phys. Rev. Lett.* **80** (1998), 660-665
 125 doi:10.1103/PhysRevLett.80.660 [arXiv:hep-ex/9708015 [hep-ex]].
- 126 [4] G. Ciezarek, A. Lupato, M. Rotondo and M. Vesterinen, *JHEP* **02** (2017), 021
 127 doi:10.1007/JHEP02(2017)021
- 128 [5] P.A. Zyla *et al.* [Particle Data Group], *PTEP* **2020** (2020) no.8, 083C01
 129 doi:10.1093/ptep/ptaa104
- 130 [6] E. McLean, C. T. H. Davies, J. Koponen and A. T. Lytle, *Phys. Rev. D* **101** (2020)
 131 no.7, 074513 doi:10.1103/PhysRevD.101.074513 [arXiv:1906.00701 [hep-lat]].
- 132 [7] C. M. Bouchard, G. P. Lepage, C. Monahan, H. Na and J. Shigemitsu, *Phys. Rev. D*
 133 **90** (2014), 054506 doi:10.1103/PhysRevD.90.054506 [arXiv:1406.2279 [hep-lat]].
- 134 [8] J. M. Flynn, T. Izubuchi, T. Kawanai, C. Lehner, A. Soni, R. S. Van de Water and
 135 O. Witzel, *Phys. Rev. D* **91** (2015) no.7, 074510 doi:10.1103/PhysRevD.91.074510
 136 [arXiv:1501.05373 [hep-lat]].
- 137 [9] A. Bazavov *et al.* [Fermilab Lattice and MILC], *Phys. Rev. D* **100** (2019) no.3, 034501
 138 doi:10.1103/PhysRevD.100.034501 [arXiv:1901.02561 [hep-lat]].
- 139 [10] A. Khodjamirian and A. V. Rusov, *JHEP* **08** (2017), 112
 140 doi:10.1007/JHEP08(2017)112 [arXiv:1703.04765 [hep-ph]].